Catalysis Letters Vol. 113, Nos. 1–2, January 2007 (© 2007)
DOI: 10.1007/s10562-006-9009-1

A highly active bi-crystalline photocatalyst consisting of TiO_2 (B) nanotube and anatase particle for producing H_2 gas from neat ethanol

Huang-Lin Kuo,[a] Chih-Yin Kuo,[a] Chun-Hsuan Liu,[a] Jiunn-Hsing Chao,[b] and Chiu-Hsun Lin[a],*

[a] *Department of Chemistry, National Changhua University of Education, Changhua, 500 Taiwan, ROC*
[b] *Nuclear Science and Technology Development Center, National Tsing Hua University, Hsinchu, 300 Taiwan, ROC*

Received 12 October 2006; accepted 24 November 2006

Sodium titanate nanotubes (NaTNTs) are converted into monoclinic TiO_2 (B) nanotubes by rinsing with 0.10 M HCl followed by drying at 573 K. As calcination temperature is increased to 673 K, these TiO_2 (B) nanotubes start to transform into anatase nanoparticles producing a bi-crystalline mixture consisting of TiO_2 (B) nanotubes and anatase nanoparticles. The primary particle size of the anatase particles was estimated to be around 10 nm using Scherrer equation. After being promoted with 1% Pt, this bi-crystalline material becomes a very active photocatalyst producing 20% more H_2 gas than 1% Pt/Degussa P-25 TiO_2 in the photocatalytic dehydrogenation of neat ethanol after 2 h of UV light irradiation.

KEY WORDS: sodium titanate nanotube; TiO_2 (B) nanotube; photocatalytic dehydrogenation; ethanol; hydrogen.

1. Introduction

The synthesis and characterization of one-dimension nanostructural materials are important as these materials have unique properties and numerous potential applications. There has been an intensive research effort in the synthesis of oxide nanotubes, and numerous micro- and nanotubes of inorganic oxides such as TiO_2, MnO_2, Co_3O_4, MoO_3, V_2O_5, Al_2O_3, ZrO_2, SnO_2 and SiO_2 all had been prepared. Titanium oxide nanostructural material, in particular, is of great interest due to its diverse applications in catalysis, photovoltaic cell, and semiconductor device. Recently, a hydrothermal method was developed utilizing re-crystallization of TiO_2 powder in a concentrated NaOH solution to produce a highly pure titanium oxide nanotubes [1,2]. This nanotube is later shown to be a titanate nanotube instead of titanium oxide nanotube, and its exact crystal structure is currently in dispute. The possible structure of the nanotube had been attributed to hydrogen titanates such as $H_2Ti_3O_7$ [3], $H_2Ti_2O_4(OH)_2$ [4] or lepidocrocite ($H_xTi_{2-x/4}\square_{x/4}O_4$ where $x = 0.7\square =$ vacancy) [5], or to sodium titanates such as $Na_xH_{2-x}Ti_3O_7$ [6], $Na_2Ti_2O_5H_2O$ [7] or $Na_2Ti_2O_4(OH)_2$ [8]. This nanotubular material has recently been successfully utilized as catalyst supports to prepare an active Ru (III) hydrated oxide catalyst for selective oxidation of alcohols [9] and a nano-sized Au catalyst for low temperature water–gas shift reaction [10].

In this communication, we want to report that the nanotubes prepared by re-crystallization of TiO_2 powder in a concentrated NaOH solution were sodium titanate nanotubes (NaTNTs), which could be transformed into monoclinic titanium oxide nanotubes (TiO_2 (B) nanotubes) by rinsing with 0.10 M HCl and calcining at 573 K. Furthermore, this TiO_2 (B) nanotube after being promoted with 1.0 wt% Pt is an active photocatalyst in the photocatalytic dehydrogenation of ethanol.

$$C_2H_5OH \rightarrow CH_3CHO + H_2$$

More interesting, by calcining these TiO_2 (B) nanotubes at 673 K a bi-crystalline material composed of TiO_2 (B) nanotubes and anatase particles is formed. This material can produce 20% more H_2 than the benchmark P-25 TiO_2 photocatalyst in the above photocatalytic dehydrogenation reaction. It is interesting that the well-defined morphology of a nanotubue was destructed producing a more active catalyst containing tubes and particles.

2. Experimental

2.1. Preparation of photocatalysts

To prepare NaTNTs, 1.5 g of TiO_2 powder (Aldrich) was mixed with 600 ml of 10 M NaOH in a 1.0 L perfluoroalkoxy container and kept the mixture in a silicon oil bath at 383 K for 96–168 h. The resulting paste was filtered and washed several times with deionized water, and dried at 383 K for 24 h to obtain NaTNTs. To prepare TiO_2 (B) nanotubes, the

---

*To whom correspondence should be addressed.
E-mail: chlin@cc.ncue.edu.tw

1011-372X/07/0100–0007/0 © 2007 Springer Science+Business Media, LLC

prepared NaTNTs was washed first with 0.10 M HCl solution several times, and then with deionized water until no Cl^- was detected in the filtrate with $AgNO_3$ solution. A thorough washing process should be used during preparation of these two materials, in which 1.0 g of paste was dispersed in 1000 mL of deionized water (or 0.10 M of HCl) and stirred at 300 rpm for 1.0 h with a mechanical stirrer. The calcination of these nanotubes was performed in a box furnace using a heating rate of 1 K/min and the calcination time is 3 h.

A photodepositon method was utilized to simultaneously deposit and reduce Pt on TiO_2 (B). Calculated amount H_2PtCl_6 was dissolved in an aqueous methanol solution (v/v = 1). Such Pt solution was then mixed with TiO_2 (B) nanotubes with a ratio of 1.0 g TiO_2 (B) nanotube : 1000 ml aqueous methanol solution. This solution mixture was stirred and irradiated with two 15 W UV lamps (315–400 nm, Sankyo Denki) for 12 h. After irradiation, the solution was filtered to obtain a dark-gray powder, which was washed with deionized water and dried at 383 K for 24 h to obtain Pt-promoted TiO_2 (B) nanotubes.

2.2. *Characterization of photocatalysts*

XRD spectra of NaTNTs and TiO_2 (B) nanotubes were recorded with Shimadzu Lab-X XRD-6000 spectrometer using Fe Kα X ray source (λ = 1.93604 A). A JOEL JSM-6700F field-emission scanning electron microscope (FE-SEM) was used to examine the morphology of the catalysts at different calcination temperatures. TEM experiments were performed with JEOL JEM-2010 transmission electron microscope. BET surface areas of the calcined catalysts were measured with Micromeritics ASAP 2010. A Shimazru 3560 UV-Vis spectrometer coupling with an integrating sphere was used to measure the diffused-reflectance UV-Vis spectra Sodium content of the nanotubes was estimated by the neutron activation analysis utilizing the neutron source from the THOR nuclear reactor locating at Hsinchu, Taiwan using Na_2CO_3 as the calibration standard.

2.3. *Photocatalytic activity tests*

An 80 mL quartz tube sealed with a rubber septum was used as the reactor to examine the production of H_2 gas. TiO_2 (B) nanotubes (10 mg) and neat ethanol (15.0 mL) were placed in the reactor in an ice bath and purged with Ar for 20 min to remove the dissolved O_2 in the ethanol. The suspension solution was irradiated with same UV light used in the photodeposition experiments at the ambient temperature for a different period of time. The gaseous and liquid products were analyzed utilizing a HP 6890 GC equipped with TCD and FID, respectively.

3. Results and discussion

Figure 1a is the XRD spectrum of the prepared nanotubes washed with deionized water only, and it is the same as those reported by other researchers [3–8]. The XRD spectrum in figure 1a is characterized by a titanate (200) crystal plane diffraction peak around $2\Theta = 12.6°$, which becomes hardly visible upon washing with 0.10 M HCl (figure 1b) and reappears at a higher diffraction angle ($2\Theta = 18°$, figure 1d) after calcining at 573 K. Neutron activation analysis indicates that these titanate nanotubes, washed with deionized water only, do contain sodium ions. The sodium ion concentration in the nanotubes will vary depending on the degree of washing and the sodium ion concentration in this particular sample was estimated to be 96,000 ppm. Assuming the nanotubes has a sodium trititanate structure, such Na^+ concentration is equivalent to a composition of $Na_{1.18}H_{0.82}Ti_3O_7$. The structure implies that the sodium ion is exchanged by H^+ from the slightly acidic deionized water (pH = 6.5) during washing. The ion exchange properties of these NaTNTs were reported by Li [6].

The figure 1b–e are the XRD spectra of these NaTNTs washed with 0.10 M HCl solution and calcined between 383 K and 773 K. The sodium ion content in these acid-washed nanotubes is effectively reduced to less than 100 ppm by washing with diluted HCl solution. As can be seen in figure 1b, upon acid-washing and drying at 383 K the titanate characteristic (200) peak has disappeared and (110) and (211) peaks are replaced

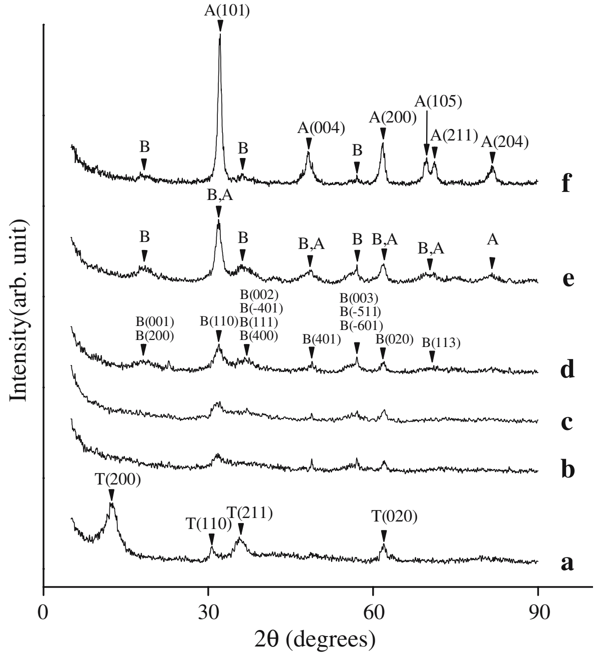

Figure 1. XRD spectra of NaTNTs for (a) washed with water and dried at 383 K, and for those washed with 0.1 M HCl and calcined at (b) 383 K, (c) 473 K, (d) 573 K, (e) 673 K, (f) 773 K. T: sodium titanate phase; B: TiO_2 (B) phase; A: anatase phase.

with new peaks of different relative intensities. Increasing the calcination temperature from 383 to 573 K improves the XRD peak intensities (and therefore, the crystallinity of the calcined samples) in figure 1b–d. In addition, an additional diffraction peak appears around $2\Theta = 18°$ (figure 1d) upon calcining the sample at 573 K. Although the diffraction peaks in figure 1d are weak, it is evident that this XRD diffraction pattern is very different from that of sodium titanate nanotubes in figure 1a. This new crystalline phase in figure 1d was identified to be TiO_2 (B) phase (JCPDS 35-0088).

Therefore, it is concluded that washing NaTNTs with HCl solution removes sodium ion in these nanotubes and transforms their crystal structure into hydrogen titanate, which upon calcination at 573 K converts to TiO_2 (B) phase. It should be noted that the broad diffraction peaks in figure 1a–d may be partly attributed to the random placement of these nanotubular materials (as can be observed in the FE-SEM micrographs in figure 2, see below).

More interestingly, as the calcination temperature is raised to 673 K, anatase phase starts to appear in the calcined mixture. This can be inferred by comparing XRD spectra in figure 1d and e. The theoretical XRD peak intensity ratio of (110) plane/(002) plane in TiO_2 (B) should be 100/90, but this ratio in figure 1e for the mixture calcined at 673 K is much higher than the theoretical value. This is no surprise as the literatures had indicated that a mixture of TiO_2 (B) and anatase phases could be obtained by calcining the hydrogen titanate such as $H_2Ti_3O_7$ [11,12]. The formation of anatase at 673 K, in the form of particles, was observed in the FE-SEM micrograph of the calcined mixture (see below, figure 2d). It should be noted that the crystallinity of TiO_2 (B) phase continues to improve reaching its maximum at 673 K. By further increasing the calcination temperature to 773 K, anatase phase now becomes the main constituent in the calcined mixture as indicated by the XRD spectrum in figure 1f. It should be pointed out that TiO_2 (B) phase is still present after calcining at 773 K.

FE-SEM was used to examine the morphology change of the catalysts at different calcination temperatures. Figure 2a and b are FE-SEM micrographs of

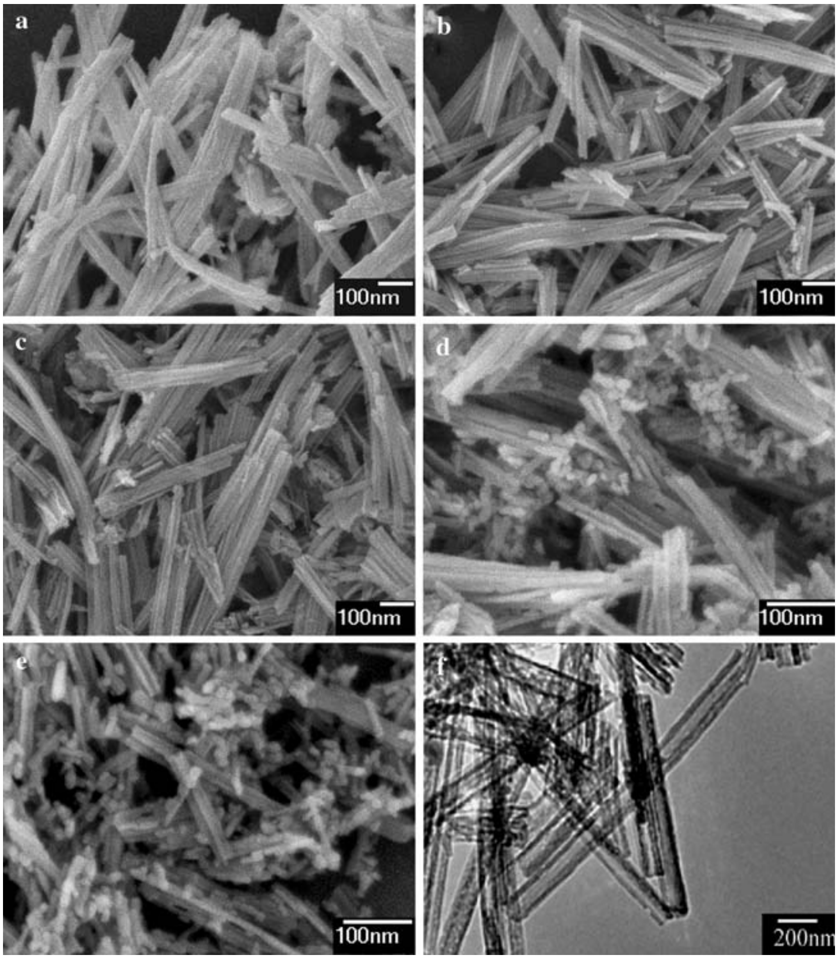

Figure 2. FE-SEM micrographs of NaTNTs (a) washed with water and dried at 383 K, and washed with 0.1 M HCl and calcined at (b) 383 K, (c) 573 K, (d) 673 K, (e) 673 K, (f) TEM micrograph for NaTNTs washed with 0.10 M HCl and dried at 383 K.

NaTNTs and acid-washed NaTNTs dried at 383 K. As can be seen from the micrographs, the appearance of these two materials looks similar and most of the materials are in the form of "nanotube bundles" as reported previously [13]. These nanotube bundles have a diameter distribution of 20–200 nm and a length distribution of 100 nm to micrometers. Figure 2f is a TEM micrograph of the NaTNTs after washing with 0.10 M HCl showing the hollow nature of these nanotubes. Raising the calcination temperature from 383 to 573 K did not produce any significant change in the morphology of the nanotube (see figure 2b, c). However, as temperature reaches 673 K, a number of particles start to appear in the calcined mixture. The formation of these anatase particles is clearly visible in the FE-SEM micrograph in figure 2d. When the calcination temperature is raised further to 773 K, the particles become the main component in the FE-SEM micrograph in figure 2f, but the tubular material is still present in the mixture.

Combining the above XRD and FE-SEM data, it is concluded that washing with 0.10 M HCl and calcining at 573 K lead to the transformation of NaTNTs into TiO_2 (B) nanotubes without any significant change in morphology. Feist had reported that heating layered hydrogen titanates at temperatures below 623 K could convert these hydrogen titanates into TiO_2 (B) [14]. Clearly, acidic washing removes Na^+ in the NaTNTs and transforms NaTNTs into hydrogen titanate nanotubes, which upon heating, are readily converted into TiO_2 (B) nanotubes starting from 383 K. Furthermore, TiO_2 (B) nanotubes are thermally stable between 383 and 573 K, and their crystallinity continues to improve with the calcination temperature. TiO_2 (B) is a polymorph of titanium oxide with a monoclinic unit cell (a = 1.21787 nm, b = 0.37412 nm, c = 0.65249 nm; β = 107.054°) [14]. It was found much earlier also by hydrothermal treatment of TiO_2 in NaOH medium by Aoki [15]. More recently, Bruce was able to selectively synthesize TiO_2 (B) nanotubes or nanowires by adjusting the hydrothermal temperature and the volume of NaOH solution used [16, 17]. As stated previously, a mixture of TiO_2 (B) and anatase phase could be obtained by calcining the hydrogen titanate such as $H_2Ti_3O_7$ [11, 12]. Therefore, further increasing the calcination temperature to 673 K, anatase TiO_2 particles started to appear in the calcined mixture. The calcined mixture is composed of a bi-crystalline mixture of TiO_2 (B) nanotubes/anatase particles. The mole fraction of TiO_2(B) in this bi-crystalline mixture calcined at 673 K is estimated to be around 33% according to the XRD spectra.

As our laboratory has an interest in utilizing this material as a photocatalyst, we have measured the diffused-reflectance UV-Vis spectra of TiO_2 (B) nanotubes calcined at different temperatures and the results are depicted in figure 3. It shows that the absorption band edges of these TiO_2 (B) nanotubes shift gradually toward the longer wavelength as the calcination temperature is increased. As a result, the ability of these TiO_2 (B) nanotubes to absorb UV ray increases with the calcination temperature. Assuming that the fundamental absorption of TiO_2 (B) nanotubes is through an indirect transition, the band gap energies of TiO_2 (B) nanotubes are obtained by plotting $(F(R)E)^{1/2}$ against E (where $F(R)$ is the Kubelka–Munk function and E is the photon energy) and extrapolating the straight line portion of the UV-Vis spectra to $(F(R)E)^{1/2} = 0$ [18]. The variation of the band gap energies (E_g) with the calcination temperature is small. The value of E_g increases slightly from 3.196 eV at 383 K to 3.225 eV at 673 K and drop to 3.204 eV at 773 K.

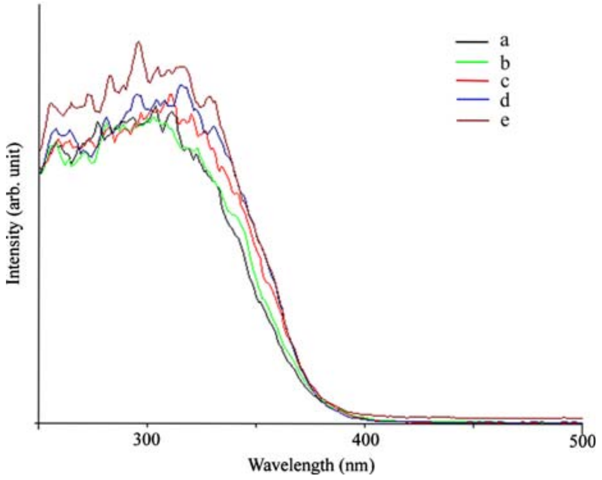

Figure 3. Diffuse-reflectance UV-vis spectra for TiO_2 (B) nanotubes calcined at (a) 383 K, (b) 473 K, (c) 573 K, (d) 673 K, (e) 773 K.

We had examined the activity of the TiO_2 (B) nanotubes calcined at different temperature for producing H_2 gas from neat ethanol in the photocatalytic dehydrogenation reaction. For the TiO_2 (B) nanotubes to be active, they need to be promoted with precious metal and 1 wt% Pt was reported to be the most effective promoter [19]. It was found that H_2 gas was the principle gas phase product with trace amount of CO_2 and CH_4 as by-products. In the liquid phase, acetaldehyde was the principle liquid phase product with a small amount of 1,1'-diethoxy ethane as the only by-product. This acetal was produced through the secondary reaction between acetaldehyde and ethanol catalyzed by the residue acidity of the TiO_2 (B) nanotubes [20]. The mole ratio of H_2/acetaldehyde is close to 1.0. This photocatalytic reaction can be summarized with the following reaction paths, where h^+ and e^- are photo-generated hole and electron, respectively.

$$TiO_2 + h\nu \rightarrow h^+ + e^-$$

$$C_2H_5OH + 2h^+ \rightarrow CH_3CHO + 2H^+$$

$$2H^+ + 2e^- \rightarrow H_2$$

$$CH_3CHO + 2C_2H_5OH \rightarrow CH_3CH(OC_2H_5)_2 + H_2O$$

$$CH_3CHO \rightarrow CH_3COOH \rightarrow CH_4 + CO_2$$

It should be pointed out that 1% Pt/NaTNTs (calcined at 673 K) produces negligible amount of H_2 (15μmol after 2 h of reaction). About 1 wt% Pt-promoted anatase particles, which are used as the starting material to prepare NaTNTs, produce only 90μmol of H_2. The same anatase particle is washed with 0.10N of HCl and then deposited with 1% Pt produces even smaller amount of H_2 (36μmol after 2 h). Figure 4 depicts the amount of H_2 gas produced by 1% Pt/TiO_2 (B) nanotubes calcined at different temperatures after 2 h of reaction. The amount of H_2 produced over 1% Pt/P-25 is also included in figure 4 for comparison. As can be observed in the figure, the amount of H_2 increases from 383 to 673 K (from 412μmol to 695μmol), but decreases slightly after calcining at 773 K (624μmol). The activity enhancement at the higher calcination temperature may be partly due to the better crystallinity and the larger band gap energy of the TiO_2 (B) nanotubes. The improvement in crystallinity can be seen from the continuous increase in diffraction peak intensities in figure 1b–e as calcination temperature is increased. Such crystallinity improvement leads to a more efficient UV ray absorption by the photocatalysts. It is well known that calcination is a very effective way to improve the photocatalytic activity of TiO_2 catalyst by improving its crystallinity through calcination [21,22]. In addition, a semiconductor with a larger band gap energy generally has a better photocatalytic activity [23].

Another important factor influencing the photocatalytic activity of this photocatalyst may be the formation of the active anatase particles in the calcined mixture. As surface areas of calcined TiO_2 (B) nanotubes are reduced from 240 m^2/g at 573 K to 132 m^2/g at 673 K (which is expected to reduce the photocatalytic activity), the material calcined at 673 K, however, is the most active photocatalyst. The crystallite size of the anatase particles produced at 673 K should be smaller than 11 nm as estimated by Scherrer equation using anatase (101) diffraction peak in figure 1f. TiO_2 with a crystallite size around 10 nm was reported to be very active in many photocatalytic reactions [24, 25]. The formation of such anatase particles is able to offset the reduction in surface area and continues to increase photocatalytic activity.

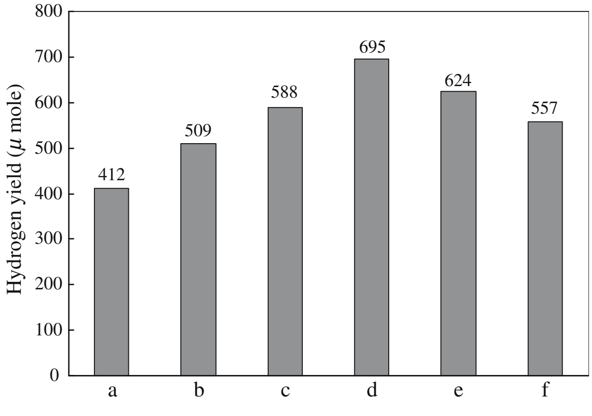

Figure 4. Hydrogen yields over 1% Pt/ TiO_2 (B) nanotubes calcined at (a) 383 K, (b) 473 K, (c) 573 K, (d) 673 K, (e) 773 K, and (f) 1% Pt/ P-25 TiO_2.

Furthermore, there is still one more possible explanation for the maximum activity for the photocatalyst calcined at 673 K is the formation of TiO_2 (B) nanotubes/anatase particles bi-crystalline material in this photocatalyst. A photocatalyst composed of two crystal phases may be beneficial to the separation of photogenerated holes and electrons, which will significantly improve the photocatalytic activity [26]. As the small anatase particles are generated from TiO_2(B) nanotubes by calcining, these two phases in the bi-crystalline mixture should have a close contact with each other as evidenced by the SEM images in figure 2. The contact points between these two phases allow for rapid electron transfer between anatase and TiO2 (B), which will facilitate the separation of photogenerated electrons and holes in this bi-crystalline titania photocatalyst.

Further raising the calcination temperature to 773 K, anatase phase became the major crystalline phase in the photocatalyst. Due to its lower surface area (99 m^2/g), a slightly smaller amount of H_2 gas was produced over this catalyst (624μmol). It needs to be pointed out that the bi-crystalline material is still present in the photocatalyst calcined at 773 K, and therefore, the photocatalyst is still very active in producing H_2. It is interesting to note that under the same condition, the benchmark 1% Pt/P-25 photocatalyst produces 557μmol of H_2, which is 20, 11, and 5% less than those produced by TiO_2 (B) nanotubes calcined at 673, 773 and 573 K, respectively. This is an interesting example that by destructing its well-defined morphology nanotubular TiO_2 could become a more active photocatalyst.

4. Conclusions

Rinsing with 0.10 M HCl and calcining at 573 K transform NaTNTs into TiO_2 (B) nanotubes with a photocatalytic activity comparable to that of P-25 TiO_2. Increasing the calcination temperature to 673 K produces a TiO_2 (B) nanotube/anatase particle bi-crystalline photocatalyst, which is able to produce 25% more H_2 gas than the benchmark P-25 TiO_2 in the photocatalytic dehydrogenation of neat ethanol. It is an interesting example that a nanotubular material has to destruct its well-define morphology in order to produce a more active catalyst.

Acknowledgments

C.-H. Lin is grateful for a grant from Nation Science Council of Taiwan (NSC-93-2113-M-018-006) and Miss Ya-Shun Lin of National ChungHsing University for the technical assistance in FE-SEM.

References

[1] T. Kasuga, M. Hiramatsu and A. Hoson, Langmuir 14 (1998) 3160.

[2] T. Kasuga, M. Hiramatsu, A. Hoson, T. Sekino and K. Niihara, Adv. Mater. 11 (1999) 1307.

[3] Q. Chen, G.H. Du, S. Zhang and L.-M. Peng, Acta Cryst. B 58 (2002) 587.

[4] M. Zhang, Z. Jin, J. Zhang, X. Guo, J. Yang, W. Li, X. Wang and Z. Zhang, J. Mol. Catal. 217 (2004) 203.

[5] R. Ma, Y. Bando and T. Sasaki, Chem. Phys., Lett. 380 (2003) 577.

[6] X. Sun and Y. Li, Chem. Eur. J. 9 (2003) 2229.

[7] C.-C. Tsai and H. Teng, Chem. Mater. 18 (2006) 367.

[8] J. Yang, Z. Jin, X. Wang, W. Li, J. Zhang, S. Zhang, X Guo, and Z. Zhang, Dalton Trans., (2003) 3898.

[9] D.V. Bavykin, A.A. Lapkin, P.K. Plucinski, J.M. Friedrich and F.C. Walsh, J. Catal. 235 (2005) 10.

[10] V. Idakiev, Z.Y. Yuan, T. Tabakova and B.-L. Su, Apply. Cataly. A: General 281 (2005) 149.

[11] X. Guo, H. Zhu, G. Pan, S. Ye, Y. Lan, F. Wu and D. Song, J. Phy. Chem. B 108 (2004) 2868.

[12] T.P. Feist, S.J. Morcarski, P.K. Davies, A.J. Jacobson and A.J. Lewandowski, Solid State Ionics 28–30 (1988) 1338.

[13] C.-H. Lin, S.-H. Chien, J.-H. Chao, C.-Y. Sheu and Y.-J. Huang, Catal. Lett. 80 (2002) 153.

[14] T.P. Feist and P.K. Davies, J. Solid State Chem. 101 (1992) 275.

[15] H. Nichizawa and Y. Aoki, J. Solid State Chem. 56 (1985) 158.

[16] A.R. Armstrong, G. Armstrong, J. Canales and P.J. Bruce, Angew Chem., Int. Ed. 43 (2004) 2286.

[17] G. Armstrong, A.R. Armstrong, J. Canales, and P.J. Bruce, Chem. Commun., (2005), 2454.

[18] M.A. Debeila, M.C. Raphulu, E. Mokoena, M. Avalos, V. Petranovskii, N.J. Coville and M.S. Scurrell, Mater. Sci. & Eng. A 396 (2005) 70.

[19] S. Teratani, J. Nakamichi, K. Taya and K. Tanaka, Bull. Chem. Soc. Jpn. 55 (1982) 1688.

[20] C.-H. Lin, C.-H. Lee, J.-H. Chao, C.-Y. Kuo, Y.-C. Cheng W.-N. Huang, H.-W. Chang, Y.-M. Huang and M.-K. Shih, Catal. Lett. 98 (2004) 61.

[21] B. Ohbtani, Y. Ogawa and S.-I. Nishimoto, J. Phys. Chem. 101 (1997) 3746.

[22] Q. Zhang, L. Gao and J. Guo, Appl. Catal. B: Environ. 26 (2000) 207.

[23] M.R. Hoffmann, S.T. Martin, W. Choi and D.W. Bahnemann, Chem. Rev. 95 (1995) 69.

[24] M. Anpo, T. Shima, S. Kodama and Y. Kubokama, J. Phys. Chem. 91 (1987) 4305.

[25] Z. Zhang, C.-C. Wang, R. Zacaria and Y.J. Ying, J. Chem. Phys. B 102 (1998) 10871.

[26] J. C. Yu, J. Yu, W. Ho, and L. Zhang, Chem. Commun. (2001) 1942.